JND Mask Adaptation for Wavelet Domain Watermarking

Mohamed Bouchakour, Guillaume Jeannic, Florent Autrusseau

Cover Page

1) Title of the paper:

JND MASK ADAPTATION FOR WAVELET DOMAIN WATERMARKING

2) authors' affiliation and address:

IRCCyN-IVC, (UMR CNRS 6597), Polytech' Nantes
Rue Christian Pauc, La Chantrerie, 44306 NANTES, France.
Tel : 02.40.68.32.47
Fax : 02.40.68.30.66

3) contact author:

Florent.Autrusseau@polytech.univ-nantes.fr

4) Conference & Publisher information:

IEEE ICME 2008
http://www.icme2008.org/
http://www.ieee.org/

5) bibtex entry:

```
@inproceedings{Bouchakour08,
	Address = {Hannover},
	Author = {M. Bouchakour, G. Jeannic, F. Autrusseau},
	Booktitle = {IEEE International Conference on Multimedia and Expo},
	Month = {June 23-26},
	Title = {JND Mask Adaptation for Wavelet Domain Watermarking},
	Year = {2008}}
```

JND MASK ADAPTATION FOR WAVELET DOMAIN WATERMARKING

Mohamed Bouchakour, Guillaume Jeannic, Florent Autrusseau

Polytech'Nantes, IRCCyN lab, rue Christian Pauc,
La Chantrerie, BP 50609, 44306 Nantes, FRANCE

ABSTRACT

One of the most challenging issues for watermarkers is to tune the strength of their watermark embedding. The strength is usually an α parameter which is increased until a reasonable trade-off between invisibility and robustness is achieved. The watermarking community needs efficient Just Noticeable Difference (JND) masks to optimally embed the watermarks. The Fourier transform is particularly adapted to the Human Visual System (HVS) modeling. In this work, we evaluate the usability of the JND mask in the wavelet domain. The use of the mask in the DWT domain involves some approximations. We will see here that the HVS decomposition and the wavelet decomposition do not perfectly fit altogether. The efficiency of the so obtained mask is tested both in terms of invisibility and robustness.

1. INTRODUCTION

It is widely admitted that among the different requirements needed in watermarking applications, the robustness and invisibility are very important. The watermark's robustness is inversely proportional to the invisibility. Thus, in watermarking context, optimising the invisibility versus robustness trade-off is crucial. Perceptual modeling is very important in watermarking context, it is in fact crucial to embed the watermark in the perceptually significant image areas, otherwise, the watermark wouldn't resist to lossy compression. Of course, as many studies have been conducted on the design of perceptual models for image compression techniques, several DCT or DWT based perceptual masks can be found in the watermarking literature [6, 7]. However, most of the DCT perceptual masks are simply based on quantization matrices, and do not take into account more complex processes, such as masking effect. One of the most advanced DCT/DWT perceptual watermarking technique was proposed by Podilchuk and Zeng [1]. The authors designed an image adaptive watermarking algorithm exploiting Watson's works for the perceptual masks implementation. Bartolini et al. have studied several perceptual masks in [4]. The first one exploited a complex multiple channels HVS model, the second was based on the local variance computation, and the last one was made from heuristic considerations. They used a bank of filters to extract an appropriate frequency range, and a Sobel filtering detecting the image edges. The authors claimed that the masks based on heuristic consideration presented better detection results than HVS based masks. The watermark weighting has always been a very challenging problem. Authors in [5] introduce the Noise Visibility Function (NVF), a content adaptive watermarking embedding scheme was designed for noise-like watermarking embedding. However very few complex HVS models are used for watermarking purpose. Evidently, an important drawback of HVS models lie in their complexity. Providing to the watermarking community an efficient (HVS based) low complexity JND mask remains an open challenge.

The goal of this paper is to adapt a previously designed JND mask in the wavelet domain. Effectively, we recently proposed in [2] a JND mask based on quantization noise visibility thresholds, and an adaptation of the mask in a Fourier domain embedding technique. As we will see in section 2 there are some incompatibilities between the Fourier splitting of the human visual system model and the Fourier representation of the wavelet sub-bands. However, as explained later, the quantization thresholds being quite similar for neighboring visual sub-bands, in this work, we spread the watermark in one DWT sub-band, and verify that most of the Fourier representation of the watermark is included within at most two neighbouring visual bands. We hereby adapt the previous embedding technique operating in the Fourier domain into the wavelets. We evaluate the efficiency of the mask regarding both invisibility and robustness. The Stirmark benchmark is used to evaluate the robustness of the proposed algorithm and PSNR, wPSNR and C4 are used to assess the quality of the marked images.

This paper is structured as follows: Section 2 presents the HVS model that we use as well as the JND mask and its adaptation to Wavelets. In section 3 we present the adaptation into wavelets and the embedding technique. Finally, section 4 gives experimental results for both in-

This work is partially supported by the ANR-Safimage project

visibility and robustness.

2. HUMAN VISUAL SYSTEM MODEL

Based on psychophysics experiments conducted in our lab, we have derived a Perceptual Channel Decomposition (PCD). The filters of the PCD are similar to the cortex filters developed by Watson. Interested reader may refer to [2] for further details on the HVS model and JND masks. As pointed out in [3], there are some incompatibilities between the HVS models decompositions and Wavelet sub-bands. Effectively, in the Fourier spectrum, sub-bands at 30° and 150° are treated separately along the visual pathways, and processed by different cells in the visual cortex, whereas, in the DWT domain this information is grouped into the same HH sub-band. As a consequence, for example, modeling the self-masking effect in these sub-bands is limited. One coefficient in the transform domain might represent different signals at 30° and 150° which do not mask each other. The PCD, defined in cycle/degree, in the frequency domain is given Figure 1-a. Figure 1-b shows a superimposition of the wavelet tilling of the spectrum on the PCD. The wavelet frequency decomposition being defined regarding the sampling frequency, this superimposition only makes sense assuming that the image is viewed under certain viewing conditions. The local contrast for a given (m, n)

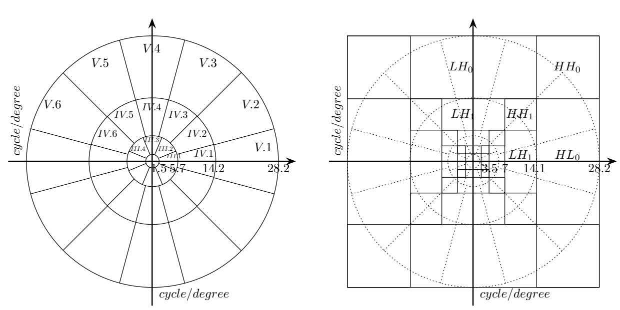

(a) Perceptual Channel Decomposition (b) Fourier splitting of the wavelet sub-bands

Fig. 1. Superimposition of perceptual channel decomposition and wavelet tiling of the spectrum.

pixel location in the i^{th} crown and the j^{th} angular channel is defined as the ratio between the luminance of the reconstructed (i, j) sub-band at the specified pixel location and the mean luminance of all the below radial sub-bands. This gives the equation 1

$$C_{i,j}(m, n) = \frac{L_{i,j}(m, n)}{\overline{L_i}(m, n)}, \tag{1}$$

where i represents the i^{th} radial channel and $\overline{L_i}(m, n)$ is the local mean luminance at the (m, n) position (i.e. spatial representation of all Fourier frequencies below the considered visual sub-band). We use the local contrast definition to determine the allowable watermark strength. Previous studies, conducted on the perceptual decomposition 1-a, determined invisible quantization conditions. Each perceptual sub-band was independently quantized and the image quality was assessed by a set of observers. The optimal quantization step (ΔC), which does not visually affect the image, has been introduced. The formula for computing the $\Delta C_{i,j}$ values can be found in [2], and Table 1 below gives the values provided by observers during subjective experiments.

	radial selectivity			
angular selectivity	LF	III	IV	V
1	0.5	0.0034	0.0066	0.026
2		0.004	0.010	0.04
3		0.0034	0.010	0.04
4		0.004	0.0066	0.026
5			0.010	0.04
6			0.010	0.04

Table 1. Experimental $\Delta C_{i,j}$ for every PCD sub-band.

3. PERCEPTUAL WATERMARKING

As previously explained, we can define the visibility of quantization noise in visual channel content for complex signals. We will now exploit this property in a watermarking context for the strength determination process. Since this model operates in a psychovisual space, the input image has to be converted into luminances (in Cd/m^2) depending on the display. The monitor's "gamma function" is used to transform the digital grey level values $N(m, n)$ into the photometric quantity known as luminance: $L(m, n) = L_{min} + L_{max} \times \left(\frac{N(m,n)}{255}\right)^{\gamma}$ where $L_{min} = 0.7$, $L_{max} = 69.3\, Cd/m^2$ and $\gamma = 1.8$. The proposed masking model suggests that we can control the visibility at each spatial site of the sub-band. So the most adequate sites of the image can be easily defined by extracting one (or several) spectrum sub-band(s). This selection may be content based, i.e. select the sub-bands of largest energy. Derived from eq. 1, the maximum watermark strength $\Delta L_{i,j}(m, n)$ allowable for each (i, j) sub-band at (m, n) pixel position, which do not induce visible artifacts is given by

$$\Delta L_{i,j}(m, n) = \Delta C_{i,j} \times \overline{L_i}(m, n). \tag{2}$$

$\Delta L_{i,j}(m, n)$ represent the JND mask computed for each (i, j) sub-band. Finally a perceptual weighting coefficient $K_{i,j}$ is computed from the watermark's spatial domain representation and the visual mask(eq. 3):

$$K_{i,j} = argmin_{m,n}\left(\left|\frac{\Delta L_{i,j}(m,n)}{W_S(m,n)}\right|\right), \tag{3}$$

where $W_S(m,n)$ is the watermark's spatial representation before weighting process by factor $K_{i,j}$ for each (m,n) spatial position. It is very important to notice that the JND masks proposed by this technique are suitable for specific frequency contents i.e. for a chosen sub-band, the frequency content of the embedded watermark should ideally be totally restrained in the same frequency content. Actually, the frequency representation of the watermark should be fully included within a PCD sub-band, whereas the corresponding JND mask is entirely made of the lower frequency disk. Restraining the watermark within a PCD sub-band is indeed easy in the Fourier domain [2], however, as previously emphasized, the wavelets sub-bands do not overlap entirely in the PCD sub-bands (Figure 1). One solution to best match the PCD, would be to embed only in the intersection of both sub-bands. A watermarking technique was designed in the DWT domain, in order to confirm the mask's efficiency to others embedding domains. A three stages wavelet transform (9/7 filters) was applied on the input image, a noise-like watermark was embedded independently in the HH_2 or LH_1. The detection technique remains the same as the one previously presented in [2]: cross-correlation is computed between the stored watermark and the extracted DWT coefficients.

4. EXPERIMENTAL RESULTS

Figure 2-a shows the spatial representation of the weighted watermark along with its Fourier representation (2-b), where the PCD is superimposed to explicitly show that most of the watermark's energy is contained within the appropriate visual sub-bands. It is important to notice on Figure 2-a that the proposed JND mask do not allow a strength adaptation in high activity areas, the watermark's strength is not increased in the image edges or textures. The JND mask being composed of weighted low frequencies (eq. 2) it provides a global watermark weighting parameter. Figure 2-c shows the variance of the watermark for each PCD sub-band (computed in the Fourier domain). This plot confirms that the frequency representation of the DWT watermark is indeed maintained in the visual sub-bands (peaks at positions 6, 7 and 11, see sub-bands numbering in Figure 2-a), and thus, the ΔC value of sub-band $(IV,1)$ can be used here for the mask implementation. As previously explained in section 3, the normalized cross-correlation is computed between the wavelet sub-band of the marked image, and the wavelet representation of the weighted

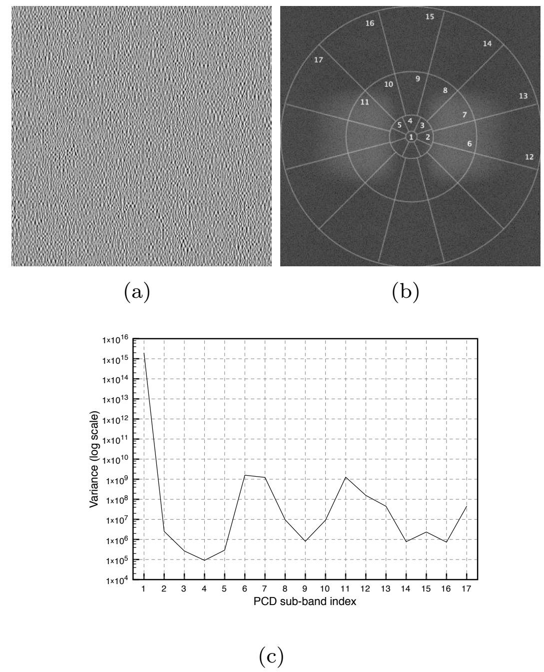

Fig. 2. (a) Spatial representation of a HL_1 watermark along with (b) its Fourier representation and (c) variance within each of the 17 PCD sub-bands.

watermark. Stirmark attacks were used to assess the robustness of the DWT embedding technique. Figure 3-b represents the cross correlation max value (Y-axis) as a function of 40 selected Stirmark attacks (X-axis). Unlike the Fourier domain embedding technique [2], the watermark is more widely spread into the frequency domain, and thus, the weighting parameter ($K_{i,j}$ in eq. 3) is sensibly lower and so are the correlation peaks (Y-axis in Figure 3-b). However, false positive and false negatives have been computed and the optimal detection threshold is set to 0.075 (dashed vertical line in Figure 3-a). The detection rate was found to be 60% for watermarks in sub-band HL_1 (dashed lines) and 80% for watermarks in HH_2 (solid lines). Effectively, as less coefficients are marked in HH_2, the strength is increased, and so is the robustness. The main goal of this work is not to propose a full DWT domain watermarking technique, but rather to adapt a spatial JND based on complex HVS properties into the wavelet domain and ensure the usability of the mask. Table 2 summarizes the quality assessment of the proposed embedding technique compared to previous works operating in the Fourier domain [2]. PSNR, wPSNR, SSIM and C4 were used (refer to [8] for details and performances of the quality metrics). We can notice on Table 2 that the quality requirements are fulfilled, all metrics present very good results. Most quality measures appeared to be better than the ones

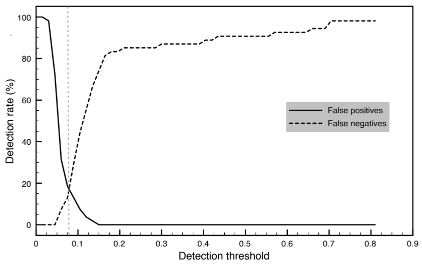

(a) False positives and False negatives rates.

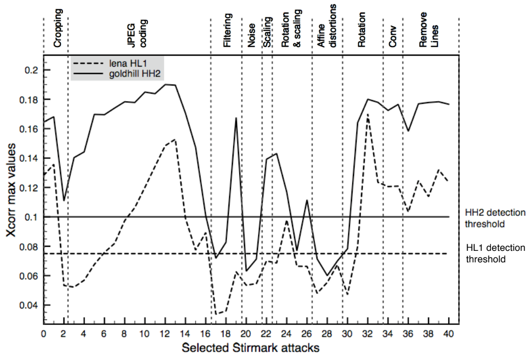

(b) Cross-correlation peaks for 40 attacks.

Fig. 3. Detection performances.

in [2], where subjective experiments were used to validate the objective scores. This slight improvement in objective quality measures is due to a wider spreading of the watermark in the Fourier frequencies. However, the wider is the watermark, the lower might be its strength. Thus the robustness performances in the DWT domain might be slightly lower than in [2]. For SSIM and C4, the closer the measure is to one, the best is the quality. Table 2 shows results for watermarked image in the HL_1 and HH_2 sub-bands. For comparison purpose, the bottom value gives results for the watermarking technique operating in the Fourier domain (8×8 watermark in sub-band $(IV, 1)$).

5. CONCLUSION

Although invisibility is a strong requirements for digital image watermarking, very few JND masks take into account advanced HVS features. Several perceptual masks based on heuristic considerations are proposed, but in order to make the embedding possible in the whole input image, including the smooth areas, complex HVS models must be considered. We proposed here an adaptation of a spatially defined JND mask into the wavelet domain. The proposed mask model have been evaluated in terms of both invisibility and robustness capabilities and showed good results regarding both requirements.

Image		PSNR	SSIM	wPSNR	C4
lena	HL_1	49.3	0.991	50.7	0.978
	HH_2	52.8	0.996	54.1	0.974
	from [2]	48.7	0.964	49.9	0.974
boats	HL_1	53.2	0.996	54.9	0.949
	HH_2	52.8	0.995	54.5	0.951
	from [2]	45.2	0.980	46.9	0.985
goldhill	HL_1	51.2	0.997	53.2	0.946
	HH_2	52.7	0.998	54.6	0.931
	from [2]	47.0	0.993	48.7	0.974
baboon	HL_1	53.2	0.996	54.9	0.986
	HH_2	52.8	0.999	57.7	0.977
	from [2]	42.8	0.992	47.5	0.978
kodie	HL_1	53.1	0.996	54.3	0.910
	HH_2	52.8	0.996	54.1	0.904
	from [2]	51.8	0.987	53.4	0.980

Table 2. Quality assessment within two distinct levels.

6. REFERENCES

[1] C. I. Podilchuk, W. Zeng, Image-adaptive watermarking using visual models, IEEE J. S. A. C., 16 (4), (1998) 525-539.

[2] F. Autrusseau and P. Le Callet, A robust image watermarking technique based on quantization noise visibility thresholds, Signal Processing, 87(6), 2007, 1363-1383.

[3] W. Zeng, S. Daly, S. Lei, An overview of the visual optimization tools in JPEG 2000, Signal Processing: Image Communication 17 (2002) 85–104.

[4] F. Bartolini, M. Barni, V. Cappellini, A. Piva, Mask building for perceptual hiding frequency embedded watermarks. Pro. of the ICIP'98, 450-454, 1998.

[5] S. Voloshynovskiy, A. Herrigel, N. Baumgaertner, T. Pun, A Stochastic approach to content adaptive digital image watermarking, Intl. Workshop on Info Hiding, LNCS 1768, 212-236, 1999.

[6] X. Huang and B. Zhang, "Perceptual Watermarking Using a Wavelet Visible Difference Predictor", Proc. of IEEE ICASSP, 2005.

[7] T. Chih-Wei and H. Hsueh-Ming, "Exploring effective coefficients in transform-domain perceptual watermarking", SPIE Electronic Imaging, Security and Watermarking of Multimedia Contents, 95-106, 2003.

[8] E. Marini, F. Autrusseau, P. Le Callet, P. Campisi, Evaluation of standard watermarking techniques, SPIE Electronic Imaging, Security, and Watermarking of Multimedia Contents, 2007.